An electron energy loss spectroscopy and electron diffraction study of the *Pmnb* polymorph of Li_2MnSiO_4

R.J. Gummow, M.G. Blackford, G.R. Lumpkin, Y. He

PII: S0925-8388(12)01974-3
DOI: http://dx.doi.org/10.1016/j.jallcom.2012.11.013
Reference: JALCOM 27236

To appear in:

Received Date: 21 September 2012
Revised Date: 1 November 2012
Accepted Date: 2 November 2012

Please cite this article as: R.J. Gummow, M.G. Blackford, G.R. Lumpkin, Y. He, An electron energy loss spectroscopy and electron diffraction study of the *Pmnb* polymorph of Li_2MnSiO_4, (2012), doi: http://dx.doi.org/10.1016/j.jallcom.2012.11.013

An electron energy loss spectroscopy and electron diffraction study of the *Pmnb* polymorph of Li_2MnSiO_4

R. J. Gummow*[a], M. G. Blackford[b], G. R. Lumpkin[b] and Y. He[a]

a. **School of Engineering and Physical Sciences, James Cook University, Townsville, Queensland, Australia 4811**

b. **Institute of Materials Engineering, ANSTO, Locked Bag 2001, Kirrawee, NSW, Australia 2232**

*** Corresponding author**

Ph: +61-7-47816223

Fax: +61-7-47816788

Email address: Rosalind.gummow@jcu.edu.au (R.J. Gummow)

Abstract

The Mn valency and the crystallinity of Li_2MnSiO_4 cathodes (*Pmnb* form) were examined with electron energy-loss spectroscopy (EELS) and selected area electron diffraction (SAED) both before and after electrochemical lithium extraction. A decrease in the crystallinity of the delithiated charged cathode particles compared to the as-prepared material was observed. The decrease in crystallinity varied from particle to particle. EELS analysis showed that the non-uniform decrease in crystallinity was due to a non-uniform extraction of lithium from the particles. The observed decrease in discharge capacity of the *Pmnb* polymorph of Li_2MnSiO_4 with cycling was attributed to the progressive loss of crystallinity and the structural collapse of Li diffusion pathways.

Keywords : electron energy loss spectroscopy; transition metal alloys and compounds; energy storage materials; crystal structure; amorphisation

1. Introduction

Research into the application of Li_2MnSiO_4 as a high-capacity lithium-ion battery cathode material is on-going despite difficulties with low electronic conductivity, polymorphism and instability of the Li_2MnSiO_4 structure on charge [1-13]. Recent results obtained from nano-structured materials produced with low temperature synthesis routes have shown vastly improved reversibility compared to bulk materials and electrochemical capacities approaching the theoretical prediction of 333 $mAhg^{-1}$ for the $P2_1/n$, $Pmn2_1$ and *Pn* polymorphs of Li_2MnSiO_4 [14-16]. Recently the *Pmnb* polymorph of Li_2MnSiO_4, earlier reported by other investigators [17, 18], has been synthesized by a facile route in

phase-pure form [19]. The difficulty in preparing this polymorph without impurities in the past has meant that it has been relatively unexplored compared to the other structural forms of Li_2MnSiO_4. The disappointing preliminary electrochemical performance of this polymorph as a cathode in Li/Li_2MnSiO_4 cells [19] was tentatively ascribed to both the poor electronic properties of the material and the likely structural collapse analogous to that of the well-described $Pmn2_1$ polymorph [20, 21].

The electron energy loss spectroscopy (EELS) spectra of lithium-transition metal compounds can be used to determine the valence state of the transition metal cations in the cathode. Since EELS spectrometers are integrated into transmission electron microscopes (TEM's), a spectrum of a nano-sized area can be obtained and can be coupled with structural data from electron diffraction spectra and composition data obtained by Energy Dispersive X-ray analysis (EDS). This combined analysis can be applied to ex-situ cathodes to give important insight into the chemical and structural changes that occur in lithium-ion battery cathode materials during electrochemical cycling [22]. EELS analysis has been applied to lithium battery cathodes including $LiMn_2O_4$ [23], $LiNi_{0.5}Mn_{1.5}O_4$ [24], $LiFePO_4$ [25-27] and the FeOF/C [28] electrode system. In this study we present both electron diffraction and EELS analysis to examine the structure and Mn valence state of ex-situ *Pmnb* Li_xMnSiO_4 ($0<x\leq2$) cathodes before and after electrochemical Li extraction in Li/Li_2MnSiO_4 cells.

2. Experimental

2.1 Synthesis and Electrochemical Delithiation of Li_2MnSiO_4

Li_2MnSiO_4 (*Pmnb* form) was synthesized by a solid-state route as detailed in [19]. Electrodes were prepared in a ratio of active material:carbon:PVDF of 60:20:20. The active material and the carbon were milled in a vibratory mill under Ar atmosphere for 2 hours using ZrO_2 grinding media. The

mixture was then mixed with PVDF dissolved in NMP and coated onto Al foil current collectors. Cathodes were dried in a vacuum drying oven at 120°C for 10 h. Swagelok test-cells were assembled in an Ar glovebox with 1M $LiPF_6$ in a 1:1 mixture by volume of ethylene carbonate and dimethyl carbonate (Merck Selectipure LP30) electrolyte. The anode was lithium foil with two discs of microporous polypropylene (Celgard 2500) as separators.

Delithiated cathodes were prepared by electrochemical extraction of lithium in Li/ Li_2MnSiO_4 cells. A typical cell was cycled at a current rate of 5 mAg^{-1} between voltage limits of 4.8 and 1.8 V in constant current mode for 2 cycles. To maintain the discharge capacity the cell was then charged in CC-CV mode to 4.8 V (charged at 5 mAg^{-1} to 4.8V and then held at 4.8V until the current decayed to $1/10^{th}$ of the initial charge current). The cell was then discharged at 5 mAg^{-1} to a lower voltage cut-off of 1.8V. This CC-CV cycling regime was used for cycles 3 and 4. Finally the cell was charge to 4.8 V in CC-CV mode as before. Cells were disassembled in an Argon glovebox and the cathodes were rinsed with DME, vacuum dried and stored in Ar for analysis.

2.2 Transmission Electron Microscopy (TEM) sample preparation and analysis

The TEM samples of the as-synthesized material were dispersed in ethanol. Drops of the dispersion were placed onto a holey carbon-coated copper grid and cleaned in Ar plasma. Charged cathodes were scraped from the current collector, dispersed in acetone and then prepared as for the as-synthesized material.

EELS spectra were collected with a Gatan GIF-2001 spectrometer attached to a JEOL 2010F field emission microscope operating at 200 keV. For EELS acquisition the spectrometer entrance aperture was set to 2 mm and the TEM operated in diffraction mode. The convergence semi-angle was 11 mrad and the collection semi-angle 28 mrad. In this configuration the energy resolution was

approximately 1.8 eV. Spectra were acquired at 0.5 eV per channel and exposure time was 0.2 sec. Spectra were recorded from areas of the specimen with thickness less than 0.5 mean free path length for inelastic scattering, therefore ZLP deconvolution was not applied.

Different techniques to quantify the L_3/L_2 intensity ratios have been used by other investigators [29-31]. In this study the background was first removed by subtracting the extrapolated pre-edge curve from the post-edge region then the continuum contribution was removed by inserting a step function as illustrated in Fig 1. After subtraction of the continuum, the white line intensities of the L_3 and L_2 lines were obtained by integration of the areas under the peaks. In agreement with the findings of Wang et al. [30] the L_3/L_2 intensity ratio was found to be a more sensitive measure of the Mn oxidation state than the absolute values of the energy positions of the edges, which are strongly affected by electromagnetic noise.

3. Results and discussion

3.1 As-prepared Li_2MnSiO_4 material

3.1.1 Selected Area Electron Diffraction (SAED) and Energy Dispersive Spectroscopy (EDS) analysis

The material used in this study is a single-phase *Pmnb* polymorph of Li_2MnSiO_4 with lattice constants a = 6.30693(2) Å, b = 10.75355(4) Å and c = 5.00863(2) Å [19]. An experimental electron diffraction (SAED) pattern and a simulated pattern down the [0, 1, -1] zone axis are shown in Fig.2a and b respectively. The experimental pattern shows a well-defined spot-pattern consistent with the *Pmnb* model. This finding was repeated with several different crystallites. Weak spots not present in

the simulated pattern and labelled dd are attributed to multiple scattering events. EDS results for the sample, collected with the TEM, gave a Si: Mn ratio of 1:0.98(3) confirming the nominal stoichiometry.

3.1.2 Electron Energy-Loss Spectroscopy (EELS)

The EELS spectra of the as-prepared Li_2MnSiO_4 (*Pmnb)* and a $MnTiO_3$ (Mn^{2+}) standard (Fig.2 c) show well-defined peaks associated with the O-K edge (525-560 eV) and the Mn L_3 and L_2 edges (630-660 eV). The intensity axis shows nominal values with the spectra displaced vertically for clarity. The energy loss and L_3/L_2 intensity ratios of the as-prepared sample agree well with the data for the Mn^{2+} standard and with results reported for Mn^{2+} oxides (Fig. 2 (c) and Table 1) [22, 32,33], confirming the Mn^{2+} oxidation state.

3.2 Electrochemically delithiated Li_2MnSiO_4

3.2.1 Electrochemical cycling and delithiation of Li_2MnSiO_4

The Li/Li_2MnSiO_4 cell used for the preparation of the delithiated cathodes (Fig. 3) gives a capacity of 254 $mAhg^{-1}$ on the first charge cycle and 113 $mAhg^{-1}$ on the first discharge to 1.8 V. The initial charge capacity agrees well with that reported earlier for the *Pmnb* material [19] but the first discharge capacity is much larger. The increase in the discharge capacity may be due firstly to the increased carbon content of 20% as opposed to 13% in the earlier experiments, secondly an increase in milling time from 1 h to 2h and lastly to the lower current rate of $5mAg^{-1}$ compared to the 20 mAg^{-1} rate reported earlier [19]. The large irreversible capacity on the first cycle may be explained by the fact that some of the initial charge capacity is likely due to side reactions of the electrode material with the electrolyte or electrolyte decomposition at the high voltages reached on charge. On the second discharge the capacity is 78 $mAhg^{-1}$. The CC-CV cycling regime, used after the first two

cycles, improves the discharge capacity on the 3rd cycle to 85 $mAhg^{-1}$ but the capacity continues to decline on the 4th cycle (75 $mAhg^{-1}$). The discontinuities in the 2nd charge and 1st discharge curves (Fig. 3) are due to unavoidable short current interruptions during the cell cycling procedure.

Detailed investigations of the *Pmn*2_1 polymorph of Li_2MnSiO_4 as a cathode in Li/Li_2MnSiO_4 cells have shown that the material loses crystallinity with cycling resulting in a collapse of the crystal structure and eventual amorphization [3, 4, 20, 21]. The observed capacity fade of the *Pmn*2_1 polymorph cathodes when cycled in Li/Li_2MnSiO_4 cells has been attributed to this mechanism. Earlier reports of SAED of partially delithiated Li_2MnSiO_4 cathodes with the *Pmn*2_1 structural form showed evidence for non-uniform amorphization. From these results it was suggested that lithium extraction from this polymorph was non-uniform and a phase separation model for lithium extraction was proposed [20]. However, no direct evidence was given for non-uniform delithiation. In this study SAED and EELS analysis of the charged *Pmnb* Li_2MnSiO_4 cathode material was undertaken to investigate whether amorphization occurs in the *Pmnb* form and whether there is any direct evidence for non-uniform lithium extraction in this case.

3.2.2 SAED and EDS

Fig. 4 (a) and (c) show the experimental SAED patterns of two adjacent particles in the charged *Pmnb* electrode TEM sample shown in the bright field image in Fig. 5. Note that, although the particles were adjacent in the TEM image, the original position of the particles in the electrode itself cannot be determined as the sample was removed from the current collector and dispersed in solvent during the TEM sample preparation procedure. The first pattern is typical of an essentially crystalline material, although the crystallinity is markedly reduced compared to the as-prepared sample (Fig 2(a)). The zone axis of the particle in Fig. 4(a) is close to [0, 2, 1]. A simulated SAED pattern of the

Pmnb form of Li_2MnSiO_4 with the [0, 2, 1] zone axis is shown if Fig. 4(b) for comparison. The second experimental SAED pattern (Fig 4 (c)) is typical of material that has been mostly amorphized – showing only two remaining well-defined spots from the residual crystalline phase and diffuse diffraction rings due to the amorphous component. These results show that, in agreement with the findings for the *Pmn*2_1 polymorph [20], there is a non-uniform loss of crystallinity when Li is extracted from the *Pmnb* form of Li_2MnSiO_4.

Li is not detectable by EDS, however the measured Mn:Si ratio of the crystalline and amorphous particles was 0.996 and 1.007, respectively. This is in close agreement with the nominal 1:1 stoichiometry for both particles.

3.2.3 EELS analysis

The EELS spectra of the Mn $L_{2/3}$ edges of the as-synthesized sample and the two charged particles are compared in Fig. 6 and Table 1. The energy scale has been shifted so that the L_3 peaks are aligned. The intensity axis is nominal and the intensities are normalized to the intensity of the L_3 peak maximum and displaced vertically for clarity. It is found that the Mn L_3/L_2 intensity ratio decreases in the charged particles indicating an increase in the Mn oxidation state [29, 30]. The more crystalline charged particle (particle 1) has a larger Mn L_3/L_2 intensity ratio than the amorphous particle (particle 2), consistent with a lower oxidation state of Mn in the crystalline particle. This gives the first direct evidence of the non-uniform extraction of lithium from the *Pmnb* form of Li_2MnSiO_4. Some particles are preferentially delithiated, becoming amorphous more rapidly, while other particles, with higher lithium content, partially retain their crystallinity. The current rate of 5mA/g used for the electrochemical cycling of the cell was low but it is possible that the use of extremely low currents may remove the observed non-uniform delithiation. Li K-edge

EELS measurements will be conducted in future studies to confirm the differences in Li content of particles with different degrees of crystallinity.

The fine structure of the O-K edges in the as-prepared, charged crystalline and charged amorphous particles (Fig. 7) shows considerable changes with Li extraction. The K_a peak at approximately 525 eV is completely absent in the as-prepared Li_2MnSiO_4 material, very poorly defined in the charged crystalline material and well-defined in the charged amorphous particle. The intensity of the pre-peak increases significantly with lithium extraction - the charged crystalline particle with a lower manganese oxidation state has a low intensity pre-peak while the charged amorphous particle with a higher manganese oxidation state has a far more intense pre-peak. This peak has been attributed by some authors to the transition of the O 1s electron to O 2p orbitals `hybridized with manganese 3d orbitals [32]. The number of available holes in the O 2p states depends on the degree of orbital hybridization with adjacent atoms. An increase in the pre-peak intensity implies more hybridization between oxygen and the surrounding atoms and an increase in the covalent nature of the bonds. One possible explanation is that, when Li is extracted from $Li_{2-x}MnSiO_4$ particles, charge compensation occurs firstly by oxidation of the Mn^{2+} cations. However, in highly delithiated particles, in addition to the oxidation of the Mn, charge compensation occurs by increased hybridization of the O-Mn bonds and a resulting decrease in the charge density around the O ions. Similar effects have been observed with the delithiated oxides $LiNi_{⅓}Mn_{⅓}Co_{⅓}O_2$ [34], $LiNi_{0.8}Co_{0.2}O_2$ [35] and $LiCoO_2$ [36]. However, studies by Jiang et al.[37] on silicate glasses have shown that the O K-edge pre-peak in their samples was not an intrinsic property of the material but was related to beam damage of the samples. Extended exposure to the beam resulted in an initial increase in the O K-edge pre-peak followed by a rapid decrease in its intensity. In this study several measurements were made on each particle and no systematic changes in the O K-edge pre-peak were observed during the process despite the increasing beam exposure time. Beam damage is therefore considered an unlikely

explanation for the observed changes in the O K-edge in this case but systematic studies of beam damage with increasing exposure time are required to completely exclude this possibility.

The energy separation of the L_3 and the O-K_a peak maxima, which has been shown to be an accurate measure of the oxidation state of manganese oxides in the 3+ to 4+ range [38], yields a calculated average manganese oxidation state of 3.5 for a typical amorphous delithiated Li_2MnSiO_4 particle. This finding was repeated with other amorphous particles. It was not possible to calculate the Mn oxidation state for the crystalline particles in this way as the O-K_a edge is absent or poorly defined in $Li_{2-x}MnSiO_4$ samples with low Mn oxidation states (Fig 7).

4. Conclusions

In this study SAED and EELS analyses of Li_2MnSiO_4 and charged Li_xMnSiO_4 samples ($x<1$) with the *Pmnb* structural form were performed. It was found that electrochemical extraction of lithium from the Li_2MnSiO_4 *Pmnb* polymorph leads to non-uniform amorphization as observed for the *Pmn*2_1 form [20]. Some particles are almost completely amorphized while others retain significant crystallinity even after 5 charge cycles. The EELS data confirmed that the non-uniform loss of crystallinity was due to non-uniform lithium extraction in the *Pmnb* form of Li_2MnSiO_4. The observed changes in the O K-edge of the delithiated samples also suggest the possibility that not all the charge compensation for lithium extraction occurs by oxidation of the Mn cations but that the O anions play a role in charge compensation in highly delithiated particles. Further studies are needed to completely exclude the possibility that some of the observed changes in the O-Kedges are due to sample damage from extended exposure to the beam.

This study has shown that, as with the *Pmn*2_1 polymorph of Li_2MnSiO_4, the crystal structure collapses when the material is cycled as a cathode in Li/Li_2MnSiO_4 cells, resulting in a destruction of

the Li ion diffusion pathways and this is the most likely explanation for the observed decrease in the discharge capacity with cycling.

Acknowledgements

AINSE is thanked for support for this research project under grant ALNGRA11120.

References

[1] V.V. Politaev, A.A. Petrenko, V.B. Nalbandyan, B.S. Medvedev, E.S. Shvetsova, J Solid State Chem, 180 (2007) 1045-1050.

[2] M.S. Islam, R. Dominko, C. Masquelier, C. Sirisopanaporn, A.R. Armstrong, P.G. Bruce, J Mater Chem, 21 (2011) 9811-9818.

[3] R. Dominko, M. Bele, A. Kokalj, M. Gaberscek, J. Jamnik, J Power Sources, 174 (2007) 457-461.

[4] R. Dominko, J Power Sources, 184 (2008) 462-468.

[5] R. Dominko, Silicates and titanates as high-energy cathode materials for Li-ion batteries, in: K.D. Nibir, S.W. Priyalal, K.D. Achyut (Eds.), SPIE, 2010, pp. 76830J.

[6] V. Aravindan, K. Karthikeyan, S. Ravi, S. Amaresh, W.S. Kim, Y.S. Lee, J Mater Chem, 20 (2010) 7340-7343.

[7] W.G. Liu, Y.H. Xu, R. Yang, Rare Metals, 29 (2010) 511-514.

[8] W.G. Liu, Y.H. Xu, R. Yang, J Alloys Compnds, 480 (2009) L1-L4.

[9] C. Deng, S. Zhang, B.L. Fu, S.Y. Yang, L. Ma, Mater Chem Phys, 120 (2010) 14-17.

[10] M.E. Arroyo-de Dompablo, M. Armand, J.M. Tarascon, U. Amador, Electrochem Commun, 8 (2006) 1292-1298.

[11] H. Duncan, A. Kondamreddy, P.H.J. Mercier, Y. Le Page, Y. Abu-Lebdeh, M. Couillard, P.S. Whitfield, I.J. Davidson, Chem Mater, 23 (2011) 5446-5456.

[12] I. Belharouak, A. Abouimrane, K. Amine, J Phys Chem C, 113 (2009) 20733-20737.

[13] R.J. Gummow, N. Sharma, V.K. Peterson, Y. He, J Power Sources, 197 (2012) 231-237.

[14] D.M. Kempaiah, D. Rangappa, I. Honma, Chem Commun, 48 (2012) 2698-2700.

[15] D. Rangappa, K.D. Murukanahally, T. Tomai, A. Unemoto, I. Honma, Nano Lett, 12 (2012) 1146-1151.

[16] A. Manthiram, T. Muraliganth, K.R. Stroukoff, Chem Mater, 22 (2010) 5754-5761.

[17] M.E. Arroyo-DeDompablo, R. Dominko, J.M. Gallardo-Amores, L. Dupont, G. Mali, H. Ehrenberg, J. Jamnik, E. Moran, Chem Mater, 20 (2008) 5574-5584.

[18] G. Mali, A. Meden, R. Dominko, Chem Commun, 46 (2010) 3306-3308.

[19] R.J. Gummow, N. Sharma, V.K. Peterson, Y. He, J Solid State Chem, 188C (2012) 32-37.

[20] A. Kokalj, R. Dominko, G. Mali, A. Meden, M. Gaberscek, J. Jamnik, Chem Mater, 19 (2007) 3633-3640.

[21] Y.X. Li, Z.L. Gong, Y. Yang, J Power Sources, 174 (2007) 528-532.

[22] F. Cosandey, Analysis of Li-ion Battery Materials by Electron Energy Loss Spectroscopy, in: A. Mendez-Vilas, J. Diaz (Eds.) Microscopy: Science, Technology, Applicationss and Education, 2010.

[23] Y. Shiraishi, I. Nakai, K. Kimoto, Y. Matsui, J Power Sources, 97-8 (2001) 461-464.

[24] N.M. Hagh, F. Cosandey, S. Rangan, R. Bartynski, G.G. Amatucci, J Electrochem Soc, 157 (2010) A305.

[25] L. Laffont, C. Delacourt, P. Gibot, M.Y. Wu, P. Kooyman, C. Masquelier, J.M. Tarascon, Chem Mater, 18 (2006) 5520-5529.

[26] P. Moreau, V. Mauchamp, F. Pailloux, F. Boucher, Appl Phys Lett, 94 (2009) 123111-1-3.

[27] P. Moreau, F. Boucher, Micron, 43 (2012) 16-21.

[28] N. Pereira, F. Badway, M. Wartelsky, S. Gunn, G.G. Amatucci, J Electrochem Soc, 156 (2009) A407-A416.

[29] T. Riedl, T. Gemming, K. Wetzig, Ultramicroscopy, 106 (2006) 284-291.

[30] Z.L. Wang, J.S. Yin, Y.D. Jiang, Micron, 31 (2000) 571-580.

[31] Z. Wang, N. Dupré, L. Lajaunie, P. Moreau, J.-F. Martin, L. Boutafa, S. Patoux, D. Guyomard, J Power Sources, 215 (2012) 170-178.

[32] H. Kurata, C. Colliex, Phys Rev B, 48 (1993) 2102-2108.

[33] J.H. Rask, B.A. Miner, P.R. Buseck, Ultramicroscopy, 21 (1987) 321-326.

[34] W.S. Yoon, C.P. Grey, M. Balasubramanian, X.Q. Yang, D.A. Fischer, J. McBreen, Electrochem Solid St, 7 (2004) A53-A55.

[35] J. Graetz, C.C. Ahn, R. Yazami, B. Fultz, J Phys Chem B, 107 (2003) 2887-2891.

[36] J. Graetz, A. Hightower, C.C. Ahn, R. Yazami, P. Rez, B. Fultz, Elec Soc S, (2003) 12-20.

[37] N. Jiang, J.C.H. Spence, Ultramicroscopy 106 (2006) 215–219.

[38] S.L. Zhang, K.J.T. Livi, A.C. Gaillot, A.T. Stone, D.R. Veblen, Am Mineral, 95 (2010) 1741-1746.

Table 1

Calculated Mn L_3/L_2 intensity ratio and Mn L_3- O K_a peak energy difference for as-synthesized and charged Li_2MnSiO_4 cathodes and standard materials for comparison.

Sample	L_3/L_2 intensity ratio	Energy difference Mn L_3 –O K_a peak maxima (eV)
$MnTiO_3$ std.(Mn^{2+})	3.8	-
Grain 1 Li_2MnSiO_4	4.3	-
Grain 2 Li_2MnSiO_4	4.2	-
Charged Grain 1 Li_xMnSiO_4	3.9	-
Charged Grain 2 Li_xMnSiO_4	1.8	112.6
MnO_2 std.(Mn^{4+})	1.9	114.05

Fig. 1

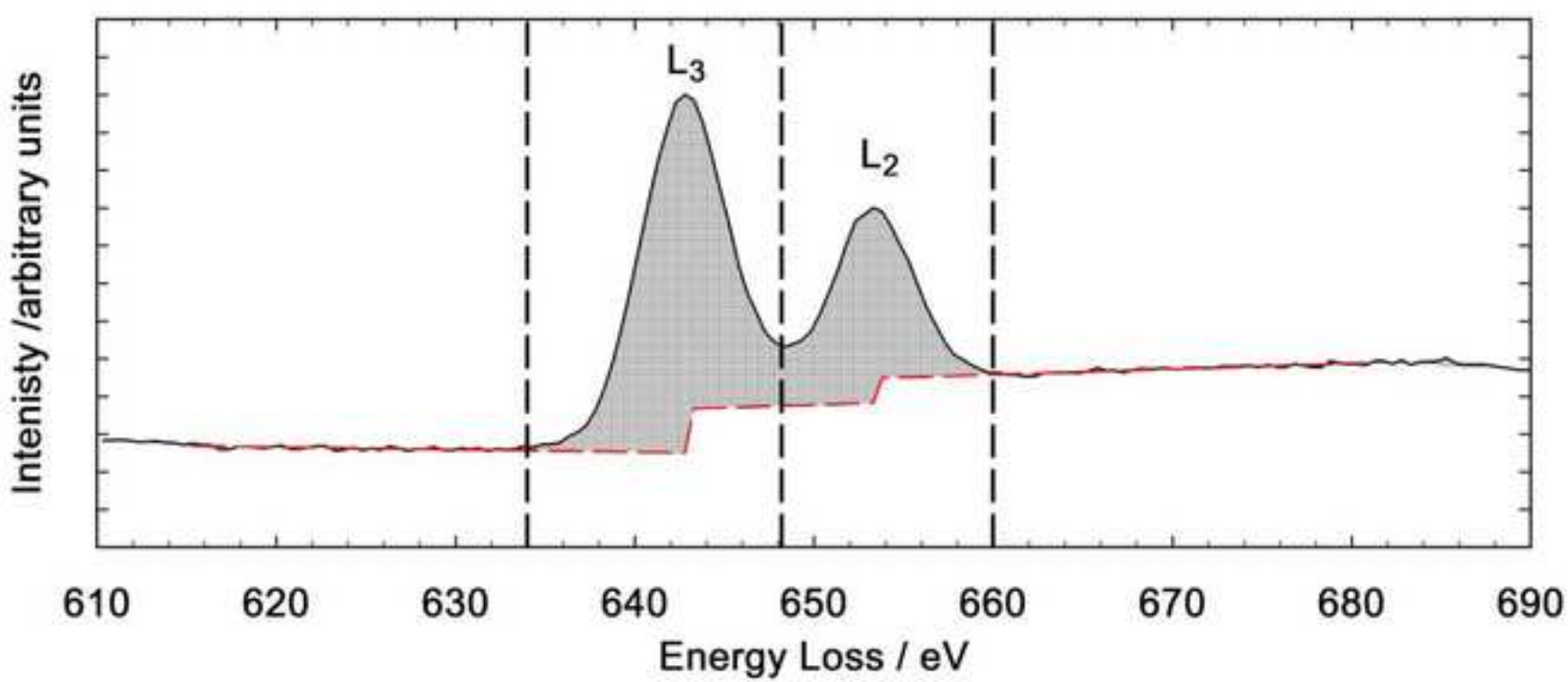

Figure(2)

Fig. 2

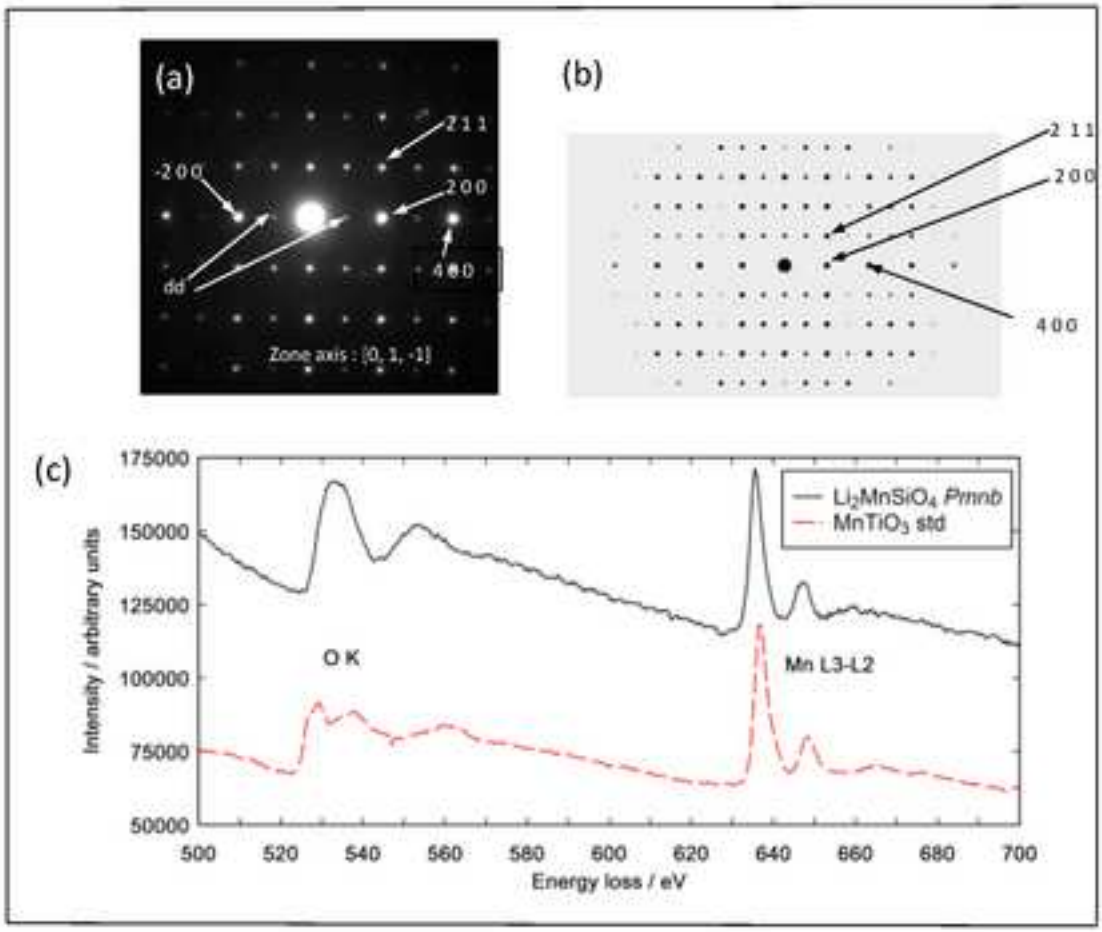

Fig. 3

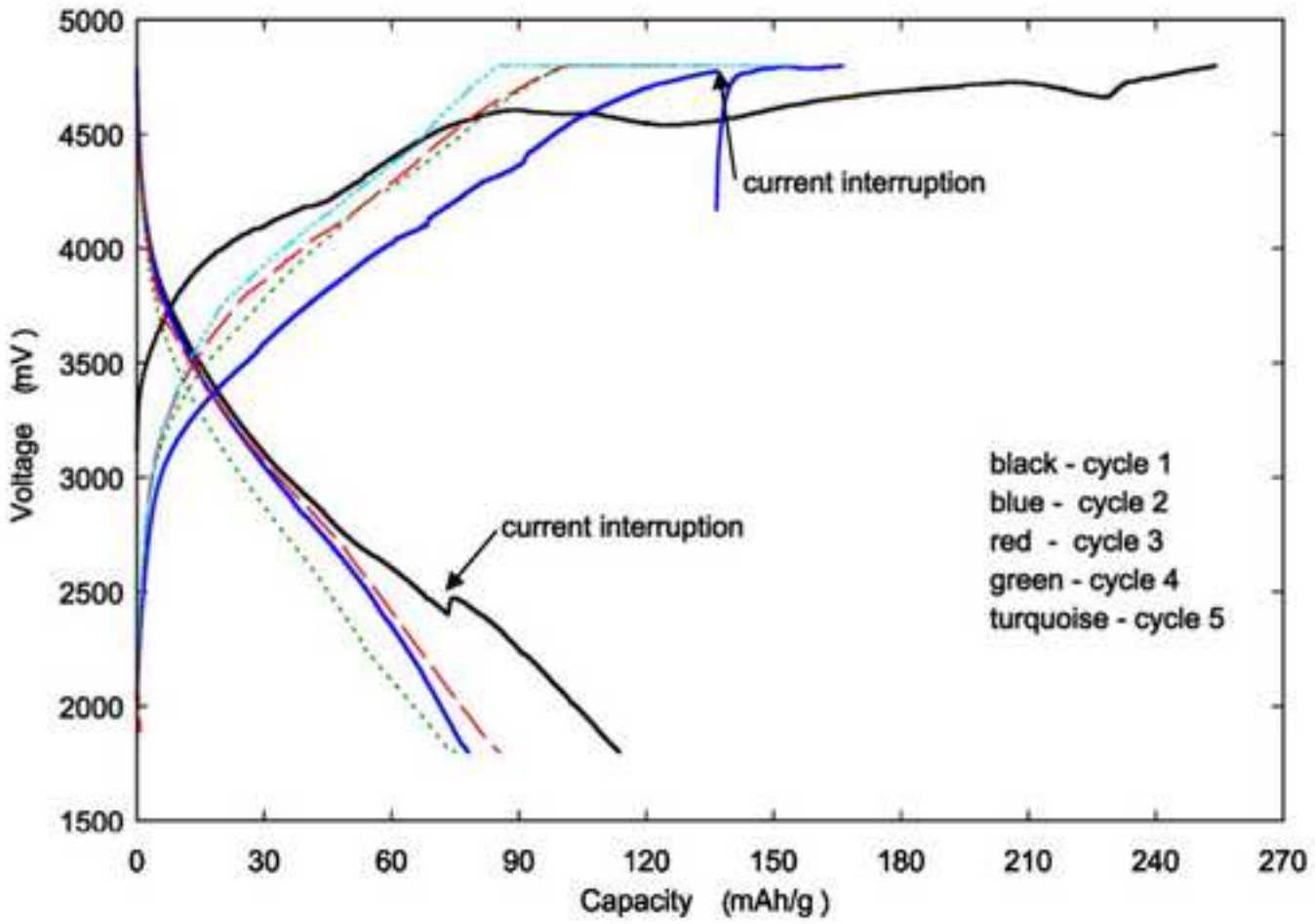

Figure(4)

Fig. 4

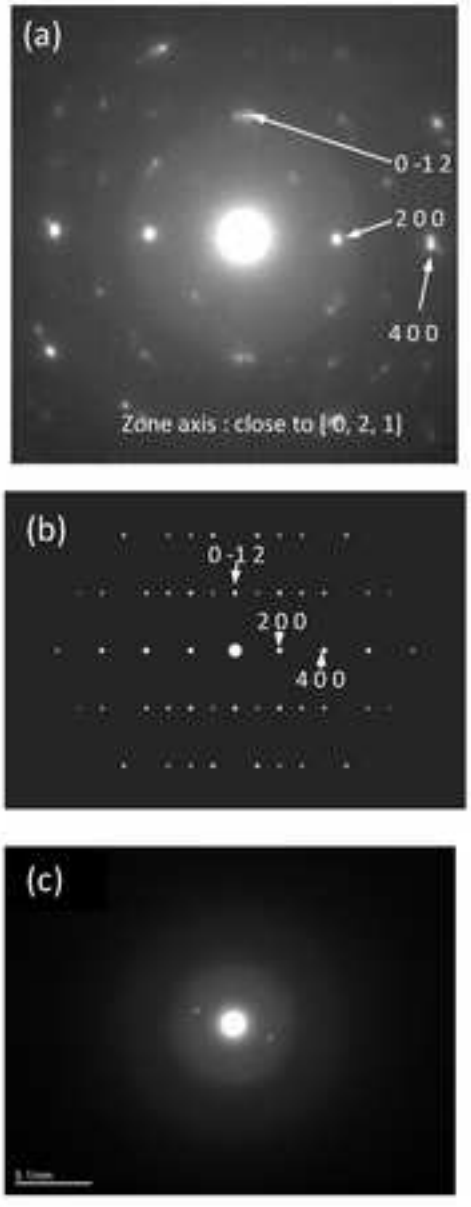

Fig. 5

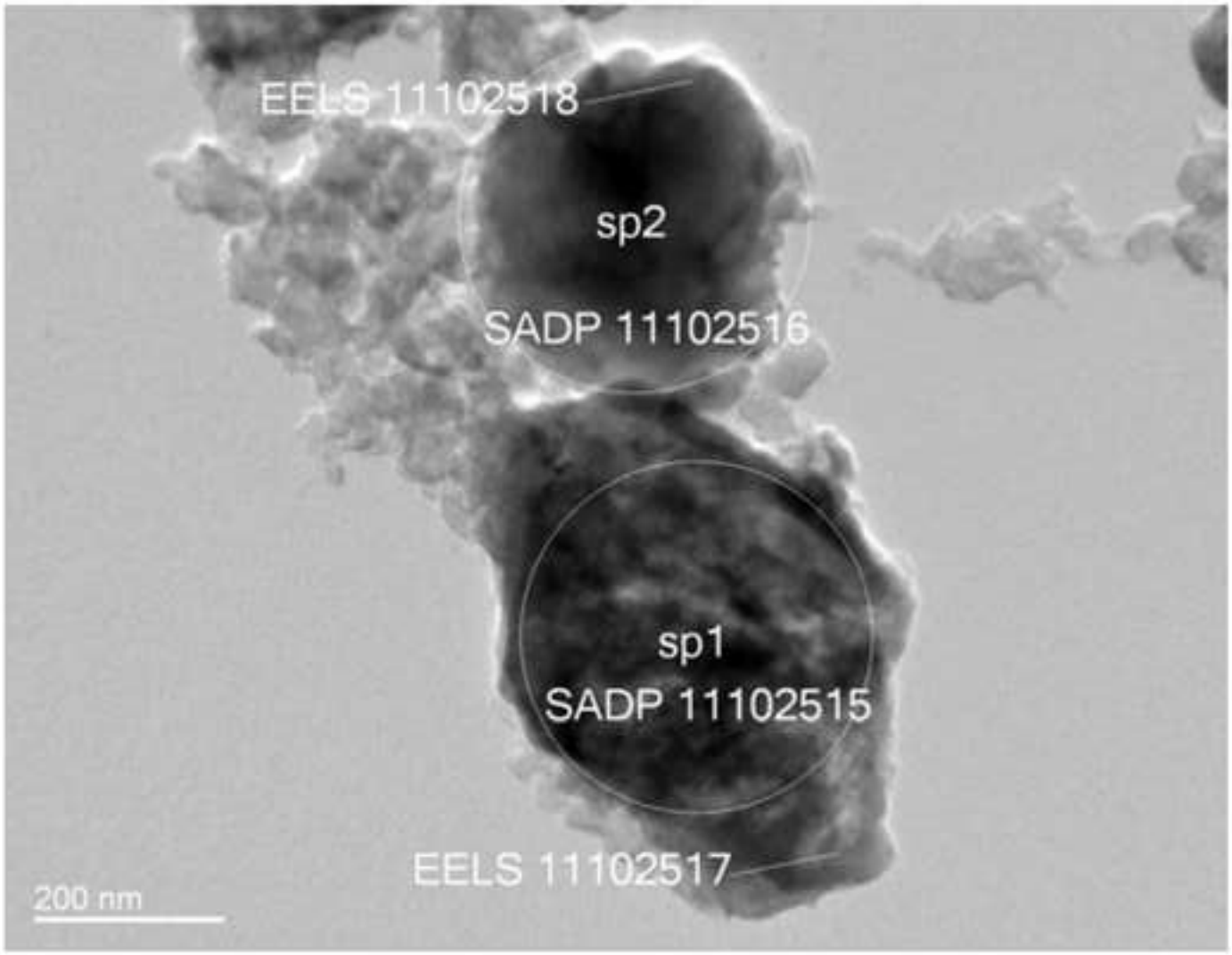

Fig. 6

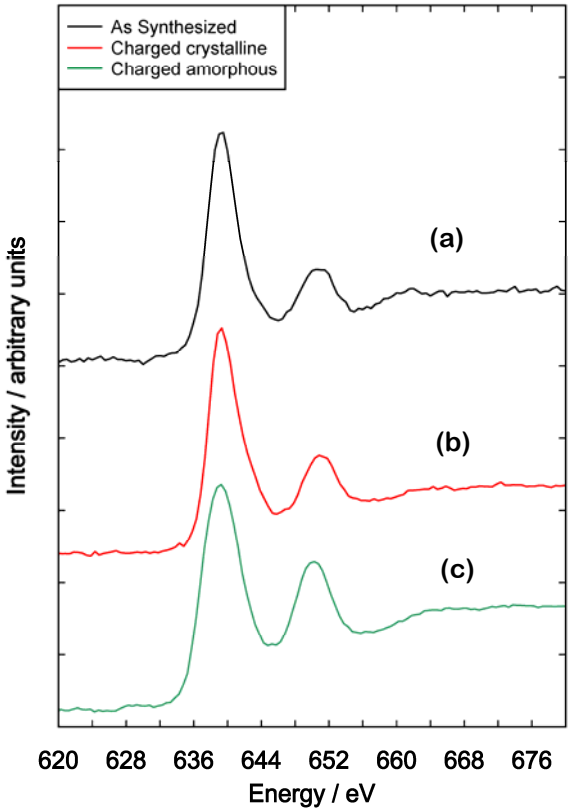
As Synthesized
Charged crystalline
Charged amorphous
(a)
(b)
(c)
Intensity / arbitrary units
620
628
636
644
652
660
668
676
Energy / eV

Fig. 7

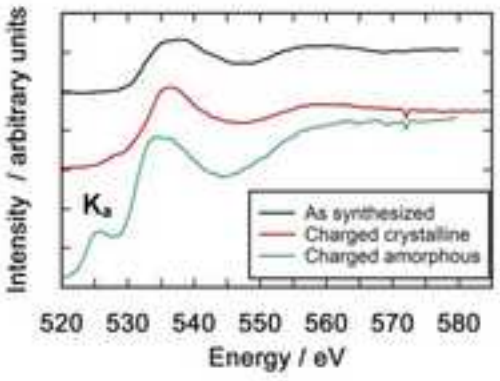

Fig. 3

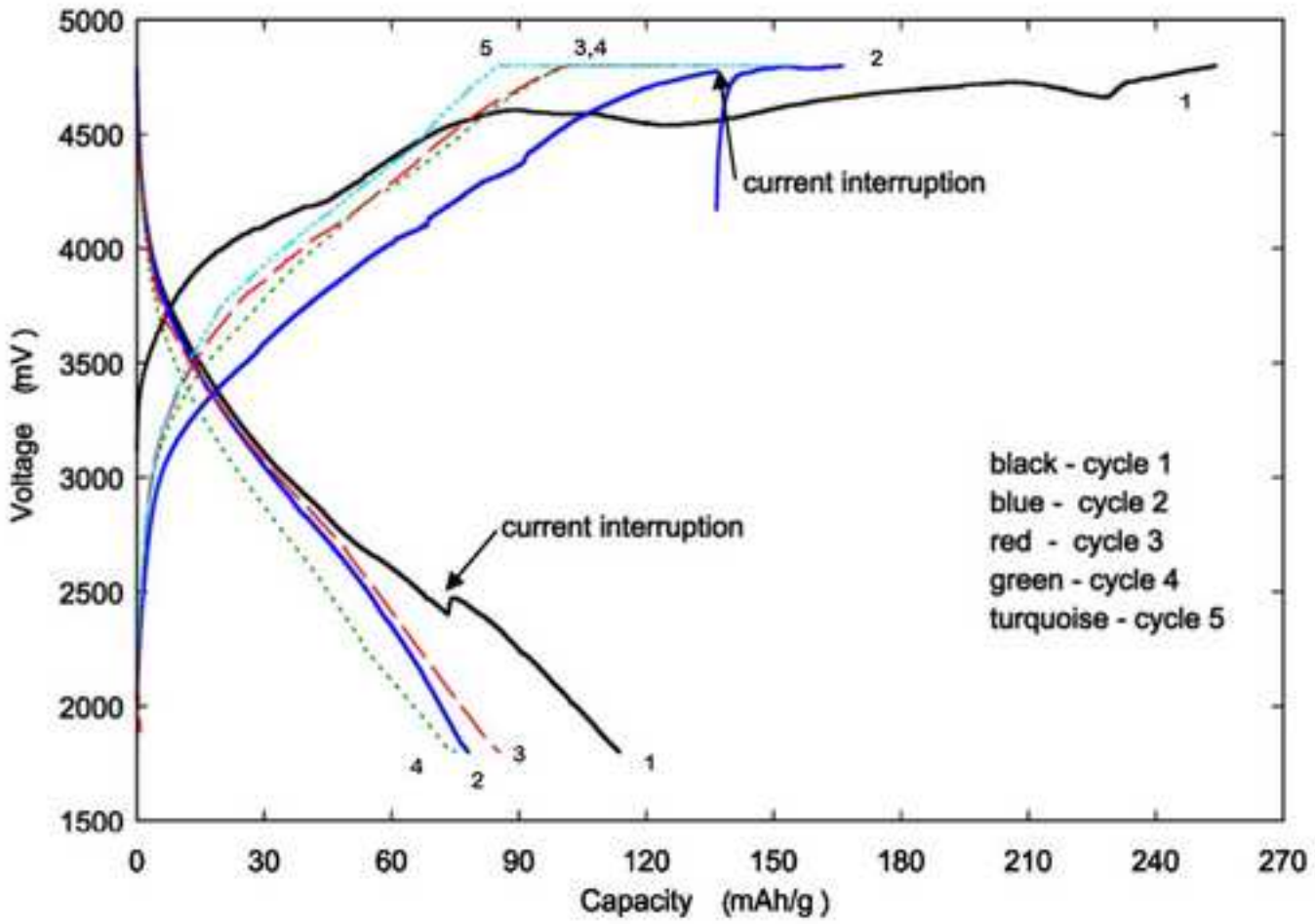

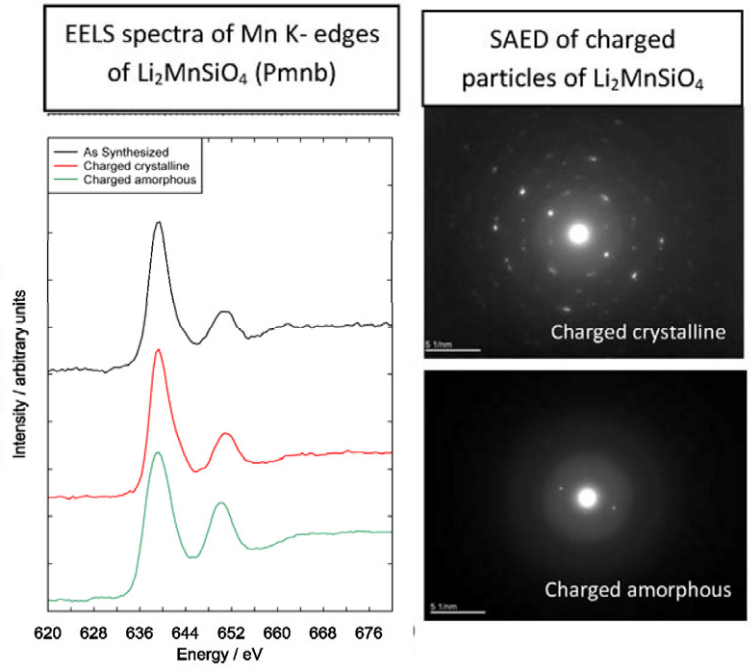

Graphical abstract

Highlights

- First EELS spectroscopy and electron diffraction of *Pmnb* polymorph of Li_2MnSiO_4.
- Capacity loss explained by electron diffraction results that showed a non-uniform loss of crystallinity in the delithiated material.
- Direct evidence for lithium extraction occurring non-uniformly in the cathode from EELS data.
- O K-edge changes possibly linked to O charge compensation for lithium loss.